Investigation of the energetic performance of pure silica BEC-type zeolite under high pressure water and 20 M LiCl intrusion-extrusion experiments

Laura Ronchi, Andrey Ryzhikov, Habiba Nouali, Jean Daou, Sebastien Albrecht, Joel Patarin

Investigation of the Energetic Performance of Pure Silica BEC-type Zeolite under High Pressure Water and 20 M LiCl Intrusion-extrusion experiments

Laura Ronchi[a], Andrey Ryzhikov[a], Habiba Nouali[a], T. Jean Daou[a,*], Sébastien Albrecht[b], Joël Patarin[a,**]

[a] Université de Strasbourg (UDS), Université de Haute Alsace (UHA), Axe Matériaux à Porosité Contrôlée (MPC), Institut de Science des Matériaux de Mulhouse (IS2M), UMR CNRS 7361, 3 bis rue Alfred Werner, F-68093 Mulhouse, France.
[b] Université de Strasbourg (UDS), Université de Haute Alsace (UHA), Laboratoire de Chimie Organique et Bioorganique (COB), EA 4566, ENSCMu, F-68093 Mulhouse, France.

ABSTRACT

The energetic performances of the pure silica BEC-type zeolite are determined by high pressure intrusion-extrusion experiments with water and 20 M LiCl electrolyte aqueous solution. BEC-type zeosil displays a bumper behavior with water and a shock absorber with 20 M LiCl aqueous solution. The characterization of the sample before and after intrusion-extrusion experiments shows clearly that the BEC structure is more affected in the presence of water than with the 20 M LiCl solution.

Keywords: Intrusion-extrusion experiment, pure silica BEC-type zeolite, energetic performances, solid-state NMR

* Corresponding author: jean.daou@uha.fr, Telephone number: +33 3 89 33 67 39, Fax number: +33 3 89 33 68 85
** Corresponding author: joel.patarin@uha.fr, Telephone number: +33 3 89 33 68 80, Fax number: +33 3 89 33 68 85

1. INTRODUCTION

Due to their unique porous properties, zeolites are used in a variety of applications with a global market of several million tons per year. The major uses are in petrochemical cracking, ion exchange, and separation and removal of gases and solvents [1]. In the last 15 years, these microporous solids and more particularly pure silica zeolites (zeosils) have been studied for applications in the energetic field [2]. This approach is based on high pressure intrusion of liquid water into the pores of zeosils, which are known to have hydrophobic properties. By submitting these porous solids to an increasing hydrostatic pressure, the intrusion of water into the pores is observed [2]. From a general point of view, during this forced penetration (intrusion), the liquid is transformed into a multitude of molecular clusters, which develop a large solid−liquid interface. The mechanical energy, spent by the pressure forces, can be converted into interfacial energy. At the microscopic scale, this phenomenon can be explained by the breaking of intermolecular bonds in the liquid to create new bonds with the solid. By reducing the pressure, the system can induce an expulsion of the liquid out of the cavities of the material (extrusion). Depending on various physical parameters related to the pore system (cavities or channels), its dimensionality (1, 2, or 3-D) or pore size, when the pressure is released the "zeosil-water" system is able to restore, dissipate, or absorb the supplied mechanical energy during the compression step, and therefore, it displays a spring, shock absorber, or bumper behavior. The energetic performances of a large number of zeosils were studied by our group and a summary of the results is reported in reference [3]. Recently this research field was extended to the intrusion of aqueous solutions of electrolytes [4-6]. Solutions of salts, such as LiCl, were demonstrated to improve the energetic performances of the "zeosil-liquid" systems by a considerable increase of the intrusion pressure. Thus, the intrusion of 20 M LiCl solution in pure silica MFI-type zeolite led to an increase of the intrusion pressure by a factor of three in comparison to pure water [4,5]. The intrusion of highly concentrated

electrolyte solutions can also change the behavior of the "zeosil- aqueous solution" system. It was the case, for instance, for the *BEA-type zeosil [6]. With water and 10 M LiCl aqueous solution, the system displays a bumper behavior, since the intruded liquid is not expelled from the solid when the pressure is released. Whereas, using concentrated LiCl aqueous solution (15-20 M) as nonwetting liquid, the system displays a shock absorber behavior and, during the decompression step, the liquid is completely expelled from the pores of the zeosil [6]. *BEA-type zeolite corresponds to an intergrown material formed by two main polymorphs A and B in variable proportions [7,8], but also a little amount of a polymorph C is proposed. This polymorph was synthesized for the first time as a germanate material named FOS-5 [9] and then as a silicogermanate (ITQ-17). [10] The structure of polymorph C in its pure silica composition was solved the first time by Liu et al.[11] but it was only observed as overgrown pillars on a Si-*BEA matrix. Then, Cantín et al. succeeded in the synthesis of the pure silica polymorph C [12]. The BEC structure code was given to this polymorph by the structure commission of the international zeolite association (IZA) [13].

BEC-type framework, as the *BEA one, is composed by a tridimensional channel system with pore openings composed by 12 tetrahedra. Channels parallel to [001] direction are interconnected to a bidimensional channel system parallel to <100> direction ([100] and [010] directions). The dimensions of the pore opening are of 6.3 x 7.5 Å and 6.0 x 6.9 Å, respectively. In contrast to polymorphs A and B, where straight and zig-zag channels are present, in polymorph C (BEC structure-type) all three 12-membered-ring channels are linear. Such a characteristic might induce differences in the energetic performances of this zeosil.

Therefore, this paper focuses on the energetic performances of BEC-type zeosil using water and 20 M LiCl aqueous solution intrusion-extrusion experiments. The BEC sample was fully characterized before and after intrusion mainly by powder X-ray diffraction, SEM, thermal analysis, N_2 adsorption-desorption and ^{29}Si NMR spectroscopy.

2. EXPERIMENTAL SECTION

2.1. Synthesis of Pure Silica BEC-type Zeolite.

The Si-BEC sample was synthesized according to the procedure published by Cantín et al.[12], using 4,4-dimethyl-4-azonia-tricyclo[5.2.2.$0^{2,6}$]undec-8-ene hydroxide as structure-directing agent (SDA). Therefore, the first step consisted in the synthesis of this SDA. The full description of its synthesis was given in SI.

For the synthesis of Si-BEC sample, the molar composition of the starting gel was : 1 SiO_2 : 0.54 SDA(OH) : 0.25 KOH : 0.54 NH_4F : 7.25 H_2O. According to the protocol described by Cantín et al. [12], Ludox AS-40 (SiO_2 40 %, Sigma-Aldrich) was mixed with 4,4-dimethyl-4-azonia-tricyclo[5.2.2.$0^{2,6}$]undec-8-ene hydroxide (SDA OH), potassium hydroxide (KOH, Fluka, assay ≥ 85 %), distilled water and ammonium fluoride (NH_4F, Sigma-Aldrich, ≥ 98 %). The gel was transferred to a 23 mL Teflon-lined stainless-steel autoclave and heated for 14 days to 175 °C. After synthesis, the product was filtered, washed with boiling distilled water and dried at 70 °C overnight. The solid was calcined under air at 600 °C for 8 hours to completely remove the organic template.

2.2. Characterization

Intrusion−extrusion experiments of aqueous solutions in the zeolite sample in the form of compressed and preliminary degassed (at 300°C under vacuum) pellets were performed at room temperature using a modified mercury porosimeter (Micromeritics Model Autopore IV), as described in our previous works [14]. The liquid phase was either pure water or saturated 20 M LiCl aqueous solution. The compressibility curve of pure water or LiCl aqueous solution was subtracted from experimental intrusion−extrusion curves. The values of the intrusion (P_{int}) and extrusion (P_{ext}) pressures correspond to that of the half volume total variation. The pressure

is expressed in megapascals (MPa) and the volume variation in milliliters (mL) per gram of calcined samples. The experimental error is estimated to 1 % on the pressure and on the volume. After intrusion−extrusion experiments, the sample intruded with LiCl was washed with water to remove traces of LiCl. The absence of chloride anions in the filtrate was controlled by adding few drops of 1 M silver nitrate aqueous solution (no silver chloride precipitate). Then the samples were dried at 70 °C overnight, and hydrated in a 80 % relative humidity atmosphere during 24 h.

X-ray powder diffraction patterns of the different samples were recorded in a Debye−Scherrer geometry on a STOE STADI-P diffractometer equipped with a curved germanium (111) primary monochromator, and a linear position-sensitive detector (6° 2θ) using Cu Kα1 radiation (λ = 0.15406 nm). Measurements were achieved for 2θ angle values in the 3−50 range, step 0.15° 2θ, and time/step = 120 s. The unit-cell parameters were determined using Louër's DICVOL91 indexing routine [15] of the STOE WinXPOW program package [16].

The size and the morphology of the crystals were determined by Scanning Electron Microscopy (SEM) using a Philips XL 30 FEG microscope.

Nitrogen adsorption−desorption isotherms were performed at -196 °C using a Micromeritics ASAP 2420 apparatus. Prior to the adsorption measurements, the samples were outgassed at 90 or 300 °C overnight under vacuum to eliminate physisorbed water. Low degassing temperature for the intruded-extruded samples was chosen to avoid the dehydroxylation process. The specific surface area (S_{BET}) and microporous volume (V_{micro}) were calculated using the BET and t-plot methods, respectively.

Thermogravimetric (TG) analyses were carried out on a TG Mettler Toledo STARe apparatus, under air flow, with a heating rate of 5 °C/min from 30 to 600 °C. As mentioned above, all samples were hydrated in 80 % relative humidity atmosphere during 24 h in order to set the hydration state.

^{29}Si MAS and ^{1}H–^{29}Si CPMAS NMR spectra were recorded on a Bruker Advance II 300 MHz spectrometer, with a double-channel 7 mm Bruker MAS probe. The recording conditions are given in Table 1.

Table 1. Recording conditions of the ^{29}Si MAS and ^{1}H–^{29}Si CPMAS NMR spectra.

	^{29}Si	
	MAS	CP MAS
Chemical shift standard	TMS[a]	TMS[a]
Frequency (MHz)	59.6	59.6
Pulse width (µs)	2.29	5.00
Flip angle	π/6	π/2
Contact time (ms)	/	8
Recycle time (s)	80	6[b]
Spinning rate (kHz)	4	4
Scans number	2000	20000

[a] TMS : TetraMethylSilane

[b] The relaxation time t_1 was optimized

3. RESULTS AND DISCUSSION

3.1. Intrusion-extrusion experiments: pressure-volume diagrams (P-V)

The P-V diagrams (intrusion-extrusion isotherms) of the “Si-BEC-water” and “Si-BEC- 20 M LiCl aqueous solution” systems are shown in Figure 1 and the corresponding characteristic data are reported in Table 2.

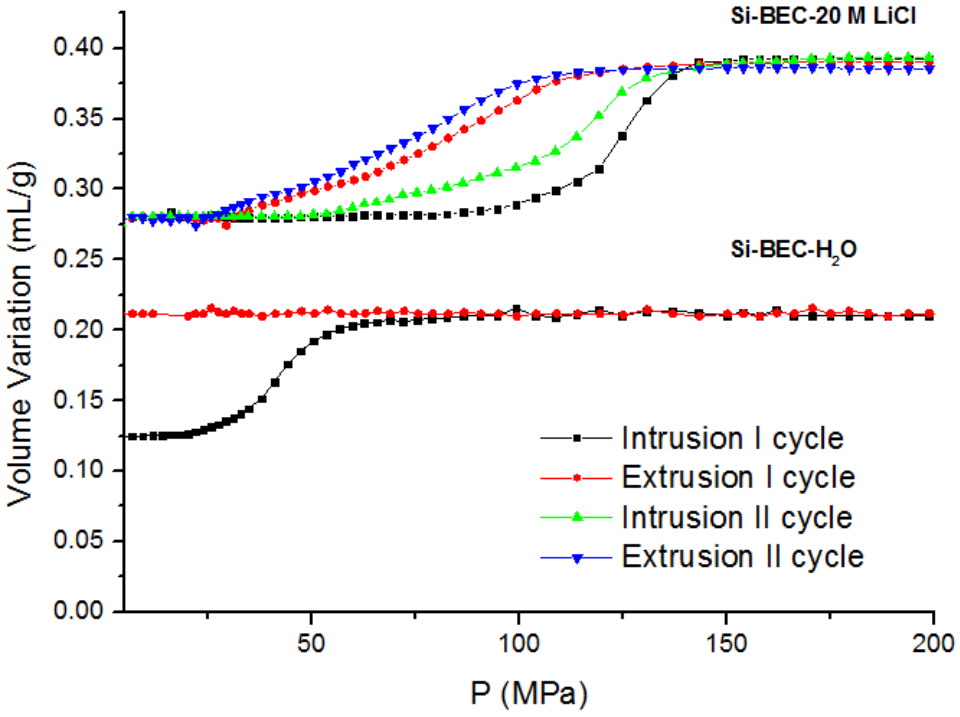

Figure 1. First intrusion-extrusion cycle of the "Si-BEC-water" system and first and second intrusion-extrusion cycles of "Si-BEC-20 M LiCl aqueous solution" system. For better visibility, intrusion-extrusion isotherms were shifted along the Y axis by 0.125 and 0.275 mL/g, respectively, and the X axis is not (350 MPa) entirely shown.

For both systems, three intrusion-extrusion cycles were performed. For clarity only the first (I) cycle is presented in Figure 1 for "Si-BEC - water" system because of the irreversible intrusion, while for "Si-BEC – 20 M LiCl aqueous solution" system two first cycles are shown. The third cycle is not shown since it is superimposable with the second one (II). The "Si-BEC - H_2O" system displays an irreversible bumper behavior and no extrusion is observed at the end of the first cycle. Water remains trapped in the porosity when the pressure is released. The "Si-BEC - 20 M LiCl aqueous solution" system, on the other hand, shows a reversible shock absorber behavior; the liquid being completely expelled from the solid at lower pressure (82 MPa). Thus, the nature of intruded liquid changes completely the system behavior. The same behaviors and the same effect were observed for *BEA-type zeosil in our previous work [6]. However the hysteresis between intrusion and extrusion isotherms is higher in the case of Si-BEC based system. In previous works on *BEA- and LTA-type zeosils the change in the system behavior

was ascribed to the different nature of the intruded liquid [6,17]. The intrusion of pure water led to a higher breaking of siloxane bridges with the formation of silanol groups that strongly interact with water molecules trapping them inside the zeolite framework. Whereas, with high concentrated LiCl solutions, water molecules solvate lithium and chloride ions and affect less the pore walls of the zeosil, thus, the solvated ions are reversibly extruded out of the pores.

Table 2. Comparison of the intrusion-extrusion parameters obtained for "Si-BEC and Si-*BEA-liquid [6]" systems. Intrusion (P_{int}) and Extrusion (P_{ext}) Pressures, Intruded (V_{int}) and Extruded (V_{ext}) Volumes, Stored (E_s) and Restored (E_r) Energies.

System	P_{int} (MPa) [a]	P_{ext} (MPa) [a]	V_{int} (ml/g) [a]	V_{ext} (ml/g)[a]	E_s (J/g) [b]	E_r (J/g) [c]	Energy Yield (%) [d]
Si-BEC-H_2O	41*	/	0.08*	/	3.3*	/	/
Si-BEC-20 M LiCl	124*/ 119**	82*/ 82**	0.11*/ 0. 11**	0.11*/ 0. 11**	13.6*/ 13.1**	9.02*/ 9.02	66*/ 69
Si-*BEA-H_2O	53*	/	0.14*	/	8.3*	/	/
Si-*BEA-20 M LiCl	115*/ 115**	103*/ 103**	0.16*/ 0.16**	0.16*/ 0.16**	18.4*/ 18.4**	16.5*/ 16.5**	90*/ 90**

[a] Determined from intrusion-extrusion isotherms.
* First cycle; ** second cycle.
[b] Stored energy $E_s = V_{int} \times P_{int}$; [c] Restored energy $E_r = V_{ext} \times P_{ext}$; [d] Energy yield = $E_r/E_s \times 100$.

For "Si-BEC zeosil – H_2O", the intrusion pressure is close to 40 MPa, while using a high concentrated LiCl solution the pressure reaches 124 MPa in the first cycle. In comparison with *BEA-type zeosil with similar structure, the intrusion pressure in BEC-type zeosil is lower for water (41 and 53 MPa for Si-BEC and Si-*BEA, respectively), but higher for 20 M LiCl solution (124 and 115 MPa for Si-BEC and Si-*BEA, respectively).

According our previous experiments such differences are correlated with the pore structure of the zeosil. For LTA-type zeosil with small 8 MR openings, the pressure increases by 7.4 times – from 20 to 149 MPa [17]. In the case of MFI-type zeosil (10 MR openings), the intrusion pressure obtained with 20 M LiCl aqueous solution was 2.9 times higher compared to that with pure water [5], while for Si-*BEA (12 MR openings) the value was only doubled (from 53 to 115 MPa – 2.2 times) [6]. However for Si-BEC with 12 MR pore openings the intrusion pressure is tripled. That shows that not only the pore size, but also the structure of the zeosil plays an important role, and even the zeosils with very close structure demonstrate a difference in energetic performances. It can be supposed that this difference between the performances of Si-BEC and Si-*BEA zeosil based systems is related with zig-zag channels which are present in *BEA structure, but absent in BEC one or with slightly different pore opening diameters (6.3 x 7.5 Å and 6.0 x 6.9 Å for BEC, 6.6 x 7.7 Å and 5.6 x 5.6 Å for *BEA).

It should be noticed that the intrusion pressure of 20 M LiCl solution is higher for the BEC-type zeosil. However, due to a lower intruded volume (0.11 (BEC) instead of 0.16 (*BEA) mL/g) because of (partially at least) the presence of 10 wt% of cristobalite (see below XRD analysis), the stored energy is lower for the "Si-BEC-20 M LiCl" system.

3.2. Characterization of the BEC samples before and after intrusion-extrusion experiments.

Prior to the analysis, the samples (before and after intrusion-extrusion experiments) were hydrated in a 80 % relative humidity atmosphere during 24 h in order to set the hydration state.

X-Ray Diffraction (XRD) analysis

The obtained XRD patterns of the samples before and after intrusion-extrusion experiments are shown in Figure 2. The XRD pattern of the nonintruded sample (Si-BEC) can be indexed in the tetragonal symmetry (space group $P4_2/mmc$). The cell parameters of the nonintruded sample

are: a = 12.599(3) Å, c = 13.127(3) Å. It is worth noting that at 21.7 2θ a non indexable peak corresponding to traces (around 10 wt %) of cristobalite is observed.

No important differences can be detected after the intrusion-extrusion tests, except a lower peak intensity. Indeed, taken the XRD peak of cristobalite as a reference peak, after intrusion-extrusion experiments, and whatever the nature of the intruded liquid (water or 20 M LiCl), the cristobalite/BEC peak intensity ratio is higher (see Figure 2 insert) revealing thus a damage of the zeolite structure. The unit-cell volume seems not to be affected after the intrusion-extrusion experiments (see Table 3).

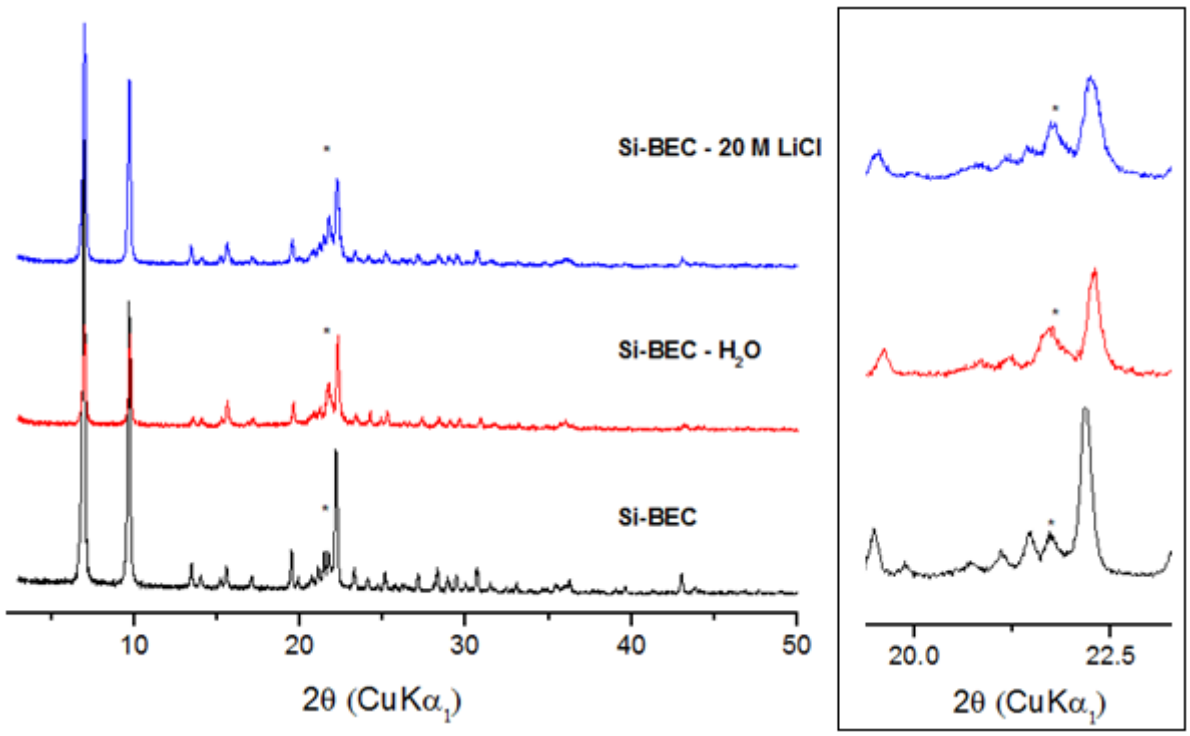

Figure 2. XRD patterns of Si-BEC samples before and after three intrusion-extrusion cycles in water and in 20 M LiCl aqueous solution. Insert: XRD in the 20-22.5 2θ range.

- **Symbol denote cristobalite peak.**

Table 3. Unit-cell parameters of Si-BEC samples before and after three intrusion-extrusion cycles in water and in 20 M LiCl solution.

Sample	***a*** **(Å)**	***c*** **(Å)**	***V*** **(Å^3)**
Si-BEC	12.599(3)	13.127(3)	2083.8(11)
Si-BEC-H_2O	12.62(9)	13.0(3)	2078.2(3)
Si-BEC-20 M LiCl	12.556(11)	13.138(9)	2071.2(36)

Scanning Electronic Microscopy (SEM) analysis

The Si-BEC samples were examined by scanning electron microscopy, before (Figure 3a) and after the intrusion-extrusion cycles (Figure 3b,c).

Two morphologies are clearly distinguishable in Figure 3a : big parallelepiped shaped crystals of Si-BEC zeolite with a size close to 0.7 x 2.5 x 0.7 μm^3 and smaller particles which might be assigned to either small crystallites of BEC-type zeolite or cristobalite. As it will be shown below from ^{29}Si MAS NMR and N_2 adsorption-desorption analysis, the estimated amount of cristobalite is close to 10 wt%.

After intrusion-extrusion experiments in water the crystals are totally damaged, while with the 20 M LiCl aqueous solution the crystals are still visible despite some damages. From these SEM micrographs, it appears that the 20 M LiCl intruded sample seems to be less affected that the intruded sample with water.

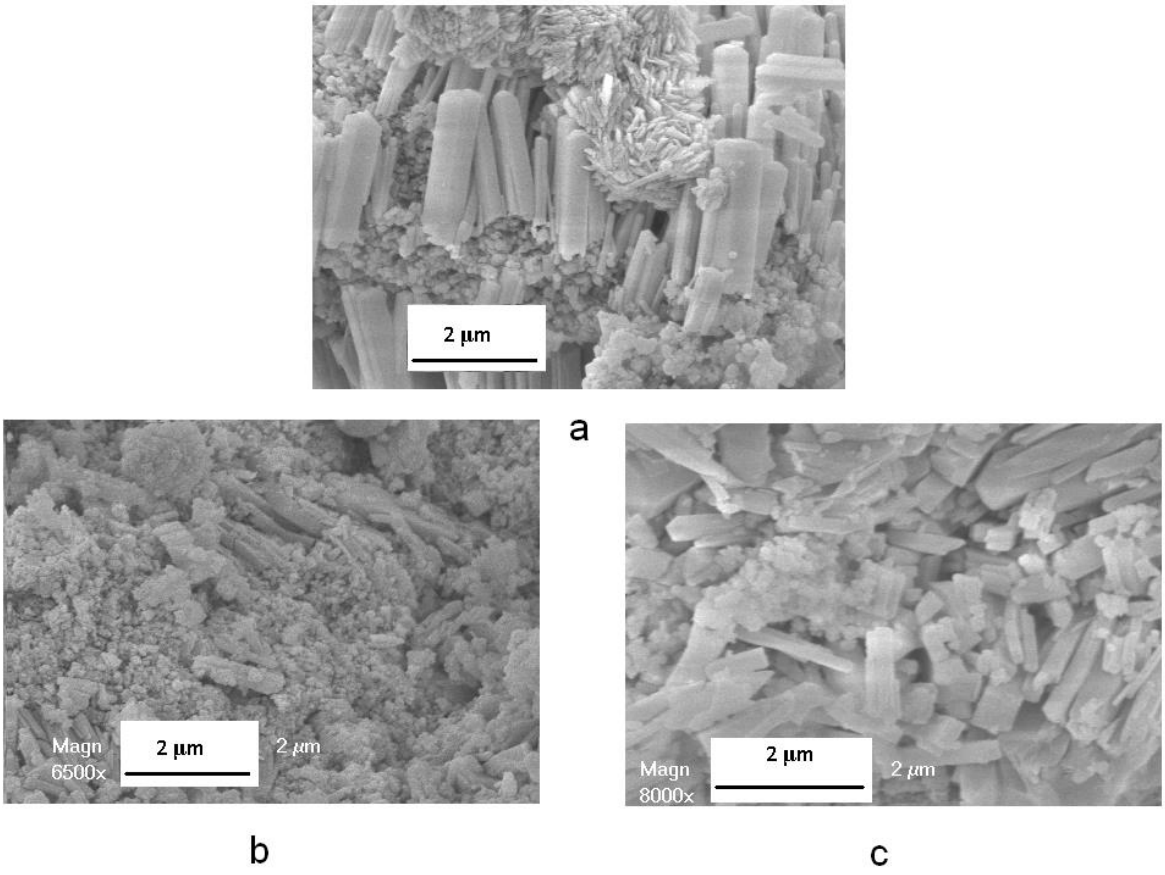

Figure 3. SEM micrographs of Si-BEC sample before a) and after three intrusion-extrusion cycles b) in water and c) in 20 M LiCl aqueous solution.

N_2 adsorption-desorption analysis

The N_2 adsorption-desorption isotherms of the nonintruded and intruded samples are shown in Figure 4 and the corresponding BET surface area (calculated for $0.000129 < p/p_0 < 0.0539$) and microporous volumes are listed in Table 4. In all cases the isotherms are mainly of type I characteristic of microporous solids. It should be noted that the nonintruded sample was outgassed at 300 °C overnight under vacuum, while the intruded samples were outgassed only at 90 °C. This temperature was chosen to eliminate physisorbed water but to avoid the dehydroxylation process.

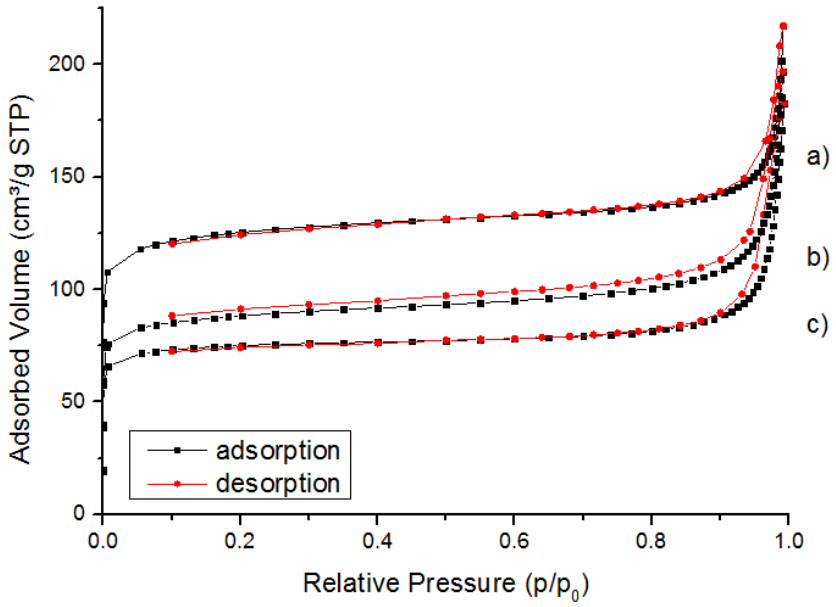

Figure 4. N_2 adsorption-desorption isotherms at 77 K of the calcined Si-BEC samples before (a) and after three cycles of intrusion-extrusion in (b) 20 M LiCl aqueous solution and (c) water.

Table 4. Values of the BET surface area and the micoporous volume obtained by N_2 adsorption-desorption isotherms at 77 K of the calcined Si-BEC sample before and after three intrusion-extrusion cycles in water and in 20 M LiCl aqueous solution.

System (outgassing temperature,°C)	S_{BET} (m^2/g)	V_{micro} (cm^3/g)
Si-BEC (300)	487	0.18
Si-BEC-H_2O (90)	295	0.11
Si-BEC-20 M LiCl (90)	343	0.13

The BET surface area and the microporous volume of the nonintruded sample are 487 m^2/g and 0.18 cm^3/g (0.2 cm^3/g in the absence of cristobalite) while for the intruded samples the corresponding values are lower (295 and 343 m^2/g; 0.11 and 0.13 cm^3/g for the water and 20 M LiCl aqueous solution intruded samples, respectively). The microporous volume values of the intruded samples are ~ 35 % lower than the nonintruded one. Even if this value is probably

overestimated (the outgassing temperature of the nonintruded sample being higher (300 °C), this indicates that defect sites have been created during the three cycles. The comparison with the textural properties of the Si-*BEA zeosil (Si-*BEA: 0.21 cm^3/g /g; Si-*BEA-H_2O: 0.10 cm^3/g g; Si-*BEA-20 M LiCl: 0.18 cm^3/g /g) [6], shows that the water intrusion leads to a higher amount of defects in the Si-*BEA framework than in the Si-BEC one, while an opposite trend is observed with the 20 M LiCl aqueous solution. This remark is confirmed by TG and NMR analysis.

Thermogravimetric analysis

The experimental results issued from the thermogravimetric (TG) analysis of the Si-BEC samples before and after intrusion-extrusion experiments are depicted in Figure 5, the corresponding data are reported in Table 5. The total weight loss ranges from 2.6 % before the intrusion-extrusion experiments to 6.8 wt % for the water intruded Si-BEC sample. The weight losses occur in two steps: the first one, situated between 30 and 150 °C, is ascribed to the desorption of physisorbed water molecules. The second one, in the temperature range of 150-600 °C, can be assigned to strongly physisorbed water molecules or more probably to water arising from dehydroxylation reactions. Whatever the intruded sample (with water or 20 M LiCl solution), this second weight loss is close to 2.2 wt% and doubled compared to the nonintruded sample (1.1 wt%). This result indicates the creation of defect sites (OH groups) after intrusion-extrusion experiments. The number of OH groups per unit cell ($Si_{32}O_{64}$) was estimated to 2.5 and 5 for the nonintruded and intruded samples, respectively. The larger number of hydrophilic OH groups in the intruded samples can explain the larger weight loss observed before 150 °C. This result is quite different from the one obtained for *BEA samples after intrusion-extrusion experiments [6]. In the latter case a drastic difference between water and 20 M LiCl intruded sample was observed, the intrusion of 20 M LiCl solution did not lead to the formation of silanol

defects. In the case of BEC-type zeosil it can be supposed that its structure is less stable, the defects are formed in both cases of water and LiCl solution intrusion-extrusion.

Table 5. Weight variation (%) of the Si-BEC samples before and after three intrusion-extrusion cycles in water and 20 M LiCl aqueous solution.

System	Weight loss (30-150 °C) wt%	Weight loss (150-600 °C) wt%	Number of OH/u.c.
Si-BEC	1.5	1.1	~ 2.5
Si-BEC-H_2O	4.6	2.2	~ 5
Si-BEC-20 M LiCl	4.0	2.2	~ 5

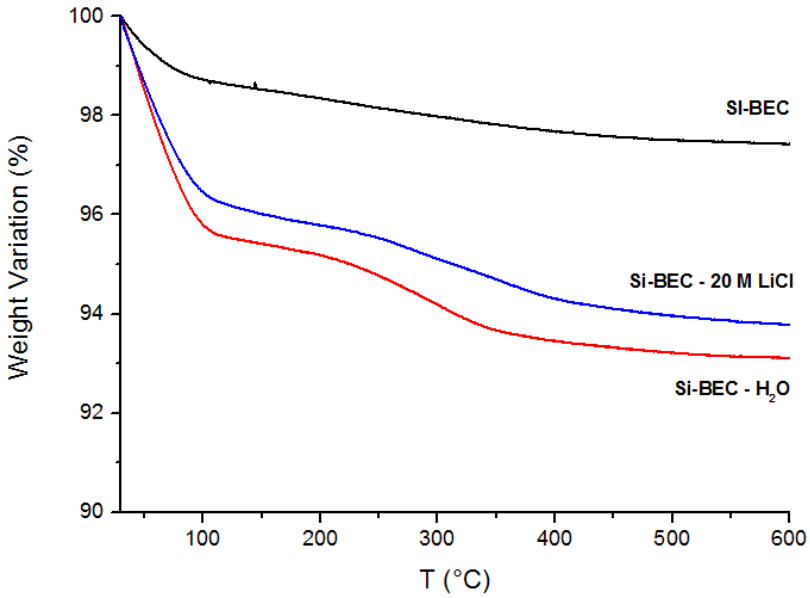

Figure 5. TG curves of the Si-BEC samples before and after three intrusion-extrusion cycles in water and 20 M LiCl aqueous solution.

As it will be confirmed by NMR spectroscopy (see below), the Si-BEC sample, similarly to the Si-*BEA sample [6], displays a hydrophobic character. The main differences between these

two zeosils can be observed after the intrusion-extrusion experiments. For the Si-BEC samples, whatever the intruded liquid (water or 20 M LiCl), defect sites are created, whereas for the Si-*BEA zeosil such sites are only created with water [6].

^{29}Si MAS NMR spectroscopy

The spectra of Si-BEC sample before and after intrusion-extrusion experiments are shown in Figure 6.

The spectrum of the nonintruded sample (left) displays three components in the -110 to -120 ppm range (-110, -112, -116 ppm) ascribed to the 3 distinct crystallographic silicon sites and corresponding to Q_4 groups. According to the site multiplicity, the area ratio of these components should be 2:1:1 (16/8/8 equivalents). From this spectrum the area ratio is close to (2.2:1:1). According to the literature [18], the cristobalite is also characterized by a main component at -110 ppm. Therefore, the slight increase observed for the intensity of the component at -110 ppm (2.2 instead of 2) can be explained by the presence of cristobalite. Its amount is quite low and estimated to 10 wt%. A very broad and small drift is slightly detectable in the -100 to -105 ppm range. It might reveal the presence of Q_3 sites (HO-Si-$(OSi)_3$ or $^-$O-Si-$(OSi)_3$); but can also be due, at least in part, to the presence of cristobalite.

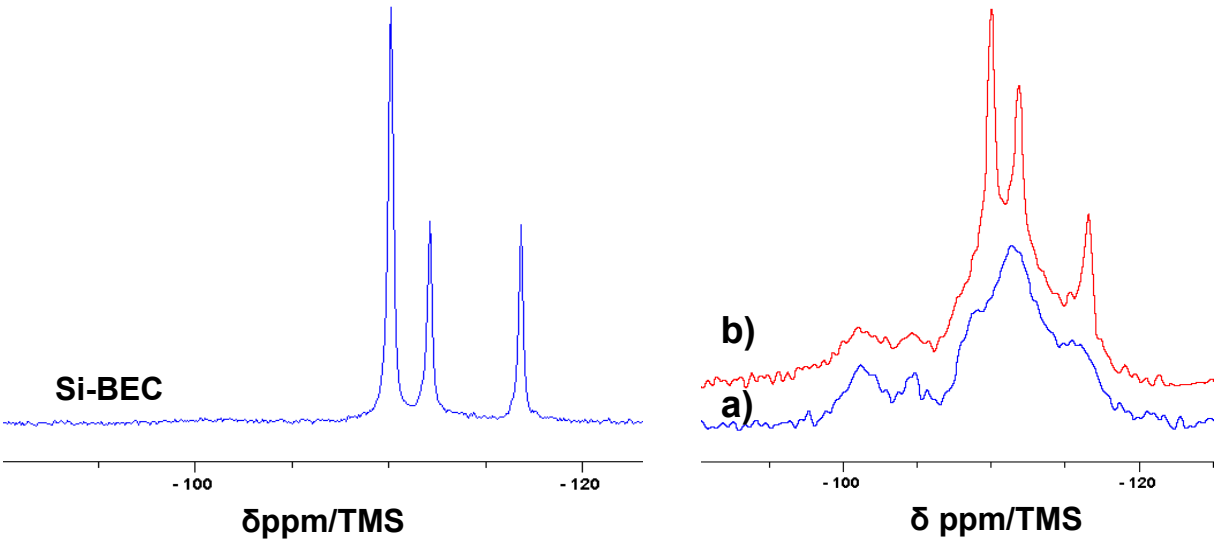

Figure 6. ^{29}Si MAS NMR spectra of the Si-BEC samples before (left) and after (right) three intrusion-extrusion cycles in (a) water and (b) 20 M LiCl aqueous solution.

After intrusion-extrusion experiments a remarkable change of the zeolite framework at the short range order is observed. For the intruded sample with water, only three broad components are detected for the Q_4 sites. For 20 M LiCl solution, an intermediate situation is observed. The three peaks assigned to Q_4 sites are clearly visible on the broad components. For both intruded samples, other two broad signals corresponding to Q_3 sites are observed. The first one at -101.1 ppm might correspond to the cristobalite phase as discussed below (see ^{1}H-^{29}Si MAS NMR section). The observation of this signal is in agreement with the XRD results described above showing a higher relative amount of cristobalite in the intruded samples probably due to a partial amorphization of the BEC structure after intrusion-extrusion experiments. This component and the other at -105 ppm might also be assigned to defect sites in the BEC structure. Such components were also observed for the Si-*BEA zeosil after intrusion with water or low concentrated LiCl aqueous solutions [6]. From these NMR spectra, it appears that the BEC structure is more affected when water is the intruded liquid. The results seem to be correlate with TG experiments where the formation of defect under water and 20 M LiCl intrusion-extrusion is observed.

^{1}H-^{29}Si CPMAS NMR spectroscopy

The spectra of Si-BEC sample before and after intrusion-extrusion experiments are shown in Figure 7.

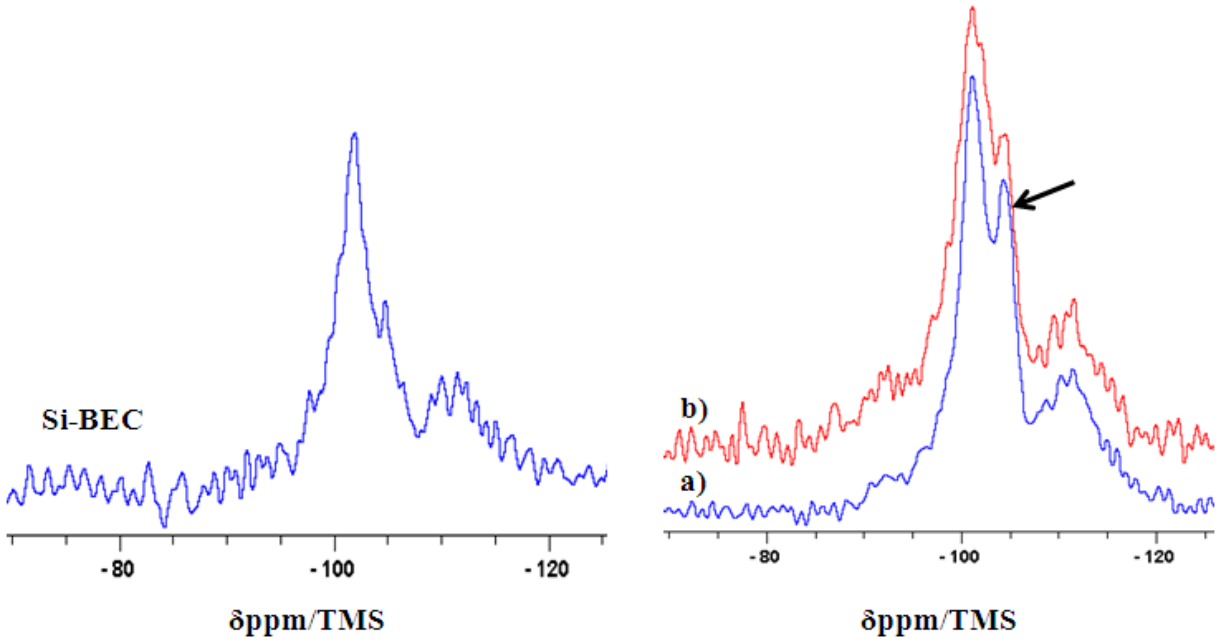

Figure 7. ^{1}H-^{29}Si CPMAS NMR spectra of the Si-BEC samples before (left) and after (right) three intrusion-extrusion cycles in (a) water and (b) 20 M LiCl aqueous solution.

^{1}H-^{29}Si CPMAS NMR does not provide quantitative results; however, it allows a relative comparison of the spectra if they were registered under the same conditions. For the nonintruded sample (Figure 7, left) the presence of a resonance at -101.1 ppm corresponding to Q_3 species is detected, in agreement with the broad drift observed in Figure 6.

Compared to the spectrum of the nonintruded sample, after intrusion-extrusion experiments the intensity of components corresponding to Q_3 sites is higher and particularly for the one at -105 ppm for the water intruded sample (see arrow, Figure 7). This result, as mentioned above, reveals a higher amount of silanol groups arising from the breaking of siloxane bridges under water intrusion.

CONCLUSION

The synthesis of pure silica BEC-type zeolite has been realized in order to compare the results of the intrusion-extrusion experiments with the already published ones of Si-*BEA [6] since the two zeosils have a very similar structure.

Unfortunately, the BEC-type zeosil was not obtained as pure phase, indeed cristobalite co-crystallizes in amount of ~ 10 wt%. Therefore, although both *BEA and BEC structures display a similar pore volume, the intruded volume for the BEC zeosil is lower than the one observed for the Si-*BEA sample, that leads to a decrease of stored energy. As it was expected from their similar structure, the two zeosils show a similar behavior during intrusion-extrusion experiments: bumper with water and shock absorber with 20 M LiCl aqueous solution. However BEC-type zeosil demonstrates lower intrusion pressure value for water (41 against 53 MPa for Si-*BEA) and higher one for 20 M LiCl intrusion (124 against 115 MPa for Si-*BEA), and also its shock absorber behavior is more pronounced (larger hysteresis between intrusion and extrusion isotherms). Thus, small differences between the zeosil structures can lead to a change of energetic performances of the "zeosil – liquid" system. N_2 adsorption-desorption, TG and NMR analysis show that the intrusion-extrusion of water leads to the formation of defect sites in Si-*BEC structure, that is in agreement with the bumper behavior of "Si-BEC – H_2O" system and the results obtained for *BEA-type zeosil. Contrary to *BEA-type zeosil, the defects are also formed under 20 M LiCl solution intrusion. However, the formation of these defects does not impact the reversible character of LiCl solution intrusion.

SUPPORTING INFORMATION

Synthesis of the structure-directing agent: (4,4-dimethyl-4-azonia-tricyclo[5.2.2.$0^{2,6}$]undec-8-ene iodide).

REFERENCES

[1] J. Čejka, H. Van Bekkum, A. Corma, F. Schüth, Introduction to Zeolite Science and Practice. Studies in Surface Science and Catalysis 168, 3rd revised ed.; Elsevier B.V.: Amsterdam, The Netherlands, 2007; p 525.

[2] V. Eroshenko, R. C. Regis, M. Soulard, J. Patarin, J. Am. Chem. Soc., 2001, 123, 8129−8130.

[3] L. Tzanis, M. Trzpit, M. Soulard, J. Patarin, J. Phys. Chem. C, 2012, 116, 20389-20395.

[4] L. Tzanis, H. Nouali, T. J. Daou, M. Soulard, J. Patarin, Mater. Lett., 2014, 115, 229-232.

[5] I. Khay, T. J. Daou, H. Nouali, A. Ryzhikov, S. Rigolet, J. Patarin, J. Phys. Chem. C, 2014, 118, 3935-3941.

[6] A. Ryzhikov, I. Khay, H. Nouali, T. J. Daou, J. Patarin, Phys. Chem. Chem. Phys., 2014, 16, 17893-17899.

[7] J. M. Newsam, M. M. J. Treacy, W. T. Koetsier, C. B. De Gruyter, Proc. R. Soc. Lond. Ser. Math. Phys. Sci., 1988, 420, 375–405.

[8] J. B. Higgins, R. B. LaPierre, J. L. Schlenker, A. C. Rohrman, J. D. Wood, G. T. Kerr, W. J. Rohrbaugh, Zeolites, 1988, 8, 446–452.

[9] T. Conradsson, M.S. Dadachov, X.D. Zou, Microporous Mesoporous Mater., 2000, 41, 183–191.

[10] A. Corma, M. T. Navarro, F. Rey, J. Rius, S. Valencia, Angew. Chem. Int. Ed., 2001, 40, 2277-2280.

[11] Z. Liu, T. Ohsuna, O. Terasaki, M. A. Camblor, M. J. Diaz-Cabañas and K. Hiraga, J. Am. Chem. Soc., 2001, 123, 5370–5371.

[12] Á. Cantín, A. Corma, M. J. Díaz-Cabañas, J. L. Jordá, M. Moliner, F. Rey, Angew. Chem. Int. Ed., 2006, 45, 8013–8015.

[13] http://www.iza-online.org/.

[14] M. Trzpit, M. Soulard, J. Patarin, N. Desbiens, F. Cailliez, A. Boutin, I. Demachy, A. Fuchs, Langmuir, 2007, 23,10131–10139.

[15] A. Boultif, D. Louër, J. Appl. Crystallogr., 1991, 24, 987-993.

[16] STOE WinXPOW, version 1.06; STOE and Cie: Darmstadt, Germany, 1999.

[17] A. Ryzhikov, L. Ronchi, H. Nouali, T. J. Daou, J.-L. Paillaud, J. Patarin, J. Phys. Chem. C, 2015, 119, 28319–28325.

[18] D. K. Murray, J. Colloid Interface Sci., 2010, 352, 163–170.